Mitochondrial Complex II Is Essential for Gametophyte Development in Arabidopsis[1][W][OA]

Gabriel León[2], Loreto Holuigue, and Xavier Jordana*

Departamento de Genética Molecular y Microbiología, Facultad de Ciencias Biológicas, P. Universidad Católica de Chile, Casilla 114–D, Santiago, Chile

Mitochondrial complex II (succinate dehydrogenase [SDH]) is part of the tricarboxylic acid cycle and the respiratory electron transport chain. Its flavoprotein subunit is encoded by two nuclear genes, SDH1-1 and SDH1-2, in Arabidopsis (Arabidopsis thaliana). The SDH1-2 gene is significantly expressed only in roots, albeit at very low level, and its disruption has no effect on growth and development of homozygous mutant plants. In contrast, SDH1-1 transcripts are ubiquitously expressed, with highest expression in flowers. Disruption of the SDH1-1 gene results in alterations in gametophyte development. Indeed, heterozygous SDH1-1/sdh1-1 mutant plants showed normal vegetative growth, yet a reduced seed set. In the progeny of selfed SDH1-1/sdh1-1 plants, distorted segregation ratios were observed, and no homozygous mutant plants were obtained. Reciprocal test crosses with the wild type demonstrated that the mutated sdh1-1 allele is not transmitted through the male gametophyte and is only partially transmitted through the female gametophyte. Consistently, microscopic analysis showed that mutant microspores develop normally until the vacuolated microspore stage, but fail to undergo mitosis I, and then cell structures are degraded and cell content disappears. On the other hand, half the mutant embryo sacs showed arrested development, either at the two-nucleate stage or before polar nuclei fusion. Down-regulation of SDH1-1 by RNA interference results in pollen abortion and a reduced seed set, as in the insertional mutant. Altogether, our results show that SDH1-1, and therefore complex II, are essential for gametophyte development.

Succinate:ubiquinone oxidoreductase (succinate dehydrogenase [SDH]; EC 1.3.5.1), commonly referred to as mitochondrial complex II, has a central role in mitochondrial metabolism as a member of both the electron transport chain and the tricarboxylic acid (TCA) cycle. This membrane-associated complex catalyzes the oxidation of succinate to fumarate and the reduction of ubiquinone to ubiquinol, and has been characterized in bacteria and heterotrophic eukaryotes (Lemire and Oyedotun, 2002; Yankovskaya et al., 2003). In these organisms, complex II contains only four subunits: two peripheral membrane proteins, a flavoprotein (SDH1) and an iron-sulfur protein (SDH2), and two small integral membrane proteins (SDH3 and SDH4). The succinate-binding site is formed by the SDH1 protein, which is covalently linked to a FAD molecule acting as acceptor of a hydride ion at an early step of succinate oxidation. This flavoprotein subunit interacts with the SDH2 subunit, which transfers the electrons to the membrane through its three nonheme iron-sulfur centers. The two integral membrane proteins, SDH3 and SDH4, anchor the SDH1-SDH2 subcomplex to the matrix side of the inner mitochondrial membrane and contain a b-type heme and the ubiquinone-binding site (Yankovskaya et al., 2003). Surprisingly, it has been shown recently that plant complex II may contain additional subunits of unknown function along with the four classical subunits (Millar et al., 2004).

SDH subunits are all encoded in the nuclear genome in Arabidopsis (Arabidopsis thaliana), just like complex II from heterotrophic eukaryotes (Scheffler, 1998; Figueroa et al., 2001, 2002; Millar et al., 2004). Surprisingly, several of the complex II subunits are encoded by more than one gene in Arabidopsis. For instance, we have reported that three nuclear genes, named SDH2-1, SDH2-2 and SDH2-3, encode the iron-sulfur subunit, and two nuclear genes, designated SDH1-1 and SDH1-2, encode the flavoprotein (Figueroa et al., 2001, 2002). SDH2-1 and SDH2-2, which have similar structures and encode nearly identical proteins, have similar expression patterns (Figueroa et al., 2001; Elorza et al., 2004). These results are consistent with the fact that SDH2-1 and SDH2-2 probably arose via a recent gene duplication event and are redundant. In contrast, we have recently reported a highly tissue-specific expression for SDH2-3: this gene, which is structurally different and would have diverged for a long time from SDH2-1 and SDH2-2, is highly expressed in the embryo during seed development and its transcript accumulates in dry seeds (Elorza et al., 2006).

SDH1-1 (At5g66760) and *SDH1-2* (At2g18450) have similar structures and encode highly similar proteins that would be functional as complex II flavoprotein since they are highly conserved when compared to their homologs in other organisms (Figueroa et al., 2002). Moreover, they contain the residues known to be involved in FAD binding and substrate binding, and in proton transfer during catalysis, and they are actively imported into isolated plant mitochondria (Figueroa et al., 2002). However, *SDH1-1* and *SDH1-2* appear to be expressed at very different levels: the *SDH1-1* mRNA was easily detected by northern-blot hybridization in all tissues examined, whereas *SDH1-2* transcripts were only detected in reverse transcription-PCR and 3′ RACE experiments (Figueroa et al., 2002).

The highest *SDH1-1* mRNA levels were found in flowers (Figueroa et al., 2002). Analogous enhanced expression in flowers has been observed for other plant nuclear genes encoding mitochondrial proteins, including *SDH2-1* and *SDH2-2*, and for mitochondrial transcripts (e.g. Huang et al., 1994; Smart et al., 1994; Heiser et al., 1996; Elorza et al., 2004). This is related to the fact that pollen development is one of the highest energy-requiring processes in plants. The most compelling evidence for an essential role of mitochondria during pollen development is the phenomenon of cytoplasmic male sterility (CMS). CMS is a maternal inherited trait in which mutations in the mitochondrial genome impair pollen development (Hanson and Bentolila, 2004). Furthermore, an increase in the number of mitochondria per cell has been reported in maize (*Zea mays*) and tobacco (*Nicotiana tabacum*) anthers during pollen development (Lee and Warmke, 1979; Huang et al., 1994).

To gain insight into the physiological role of complex II and to explore the function of the multiple genes encoding the same SDH subunit, our group has undertaken a reverse genetic analysis of the *SDH* genes. Here we report the analysis of T-DNA insertional mutants in *SDH1-1* and *SDH1-2*, the flavoprotein genes. Our results reveal that *SDH1-2* is dispensable and that the *sdh1-1* null allele behaves as a general gametophytic mutation, demonstrating that complex II plays an essential role in gametophyte development.

RESULTS

Isolation of T-DNA Insertion Mutants of Arabidopsis *SDH1* Genes

Several different mutant lines carrying T-DNA insertions in the *SDH1-2* gene were identified as described in "Materials and Methods." One mutant was isolated and further characterized: the T-DNA was confirmed to be in the eighth out of 15 exons, and interrupted codon 336. The precursor SDH1-2 polypeptide deduced from the gene sequence has 632 amino acids and disruption at codon 336 that is upstream of several residues involved in FAD and substrate binding, and

in catalysis is expected to result in a null mutation. Homozygous *sdh1-2* mutant plants were obtained and showed no apparent phenotypic defects during vegetative or reproductive growth when compared to wild-type plants, at least under the growth conditions used.

These results indicate that the loss of *SDH1-2* has no impact on Arabidopsis growth and development, a fact consistent with our previous expression data (Figueroa et al., 2002). Furthermore, data on *SDH1-2* expression in the existing large expression databases confirm that *SDH1-2* is not expressed or is expressed at a very low level in most tissues and developmental stages (Supplemental Fig. S1; Schmid et al., 2005; see also https://www.genevestigator.ethz.ch, Zimmermann et al., 2004 for microarray data; and http://mpss.udel.edu/at, Meyers et al., 2004 for Massively Parallel Signature Sequencing experiments). Significant expression was only observed in roots, nevertheless its expression level is still less than 10% that of *SDH1-1* in the same tissue (Supplemental Fig. S1).

For *SDH1-1*, only one mutant line was identified: the T-DNA insertion was mapped to exon 9 and interrupts codon 317 (Fig. 1A). The SDH1-1 precursor polypeptide has 634 amino acids and disruption at codon 317 is expected to result in a null mutation. Genotyping of T_2 plants obtained from the seed pool sent by the Arabidopsis Biological Resource Center (ABRC) led to the identification of several heterozygous *SDH1-1/sdh1-1* mutant plants (Fig. 1B). However, attempts to identify homozygous *sdh1-1/sdh1-1* mutant plants were unsuccessful. Moreover, no homozygous mutant seedlings were obtained in the progeny of selfed *SDH1-1/sdh1-1* plants, suggesting that gametophyte and/or embryo development are altered and that *SDH1-1* is an essential gene. Currently, there are no other mutant alleles available for *SDH1-1*, as confirmed by searching the Arabidopsis Insertion Data Base (http://atidb.org/cgi-perl/index).

Molecular Characterization of Heterozygous *SDH1-1/sdh1-1* Mutant Plants

Northern-blot analysis was performed using RNA from three wild-type plants and six plants carrying the *sdh1-1* mutated allele (Fig. 1C). As expected, the heterozygous mutant plants showed a reduced steady-state level of the *SDH1-1* mRNA (roughly 50%). To assess whether this transcript decrease results in a lower complex II activity, succinate:quinone reductase (SQR) activity was measured in three independent experiments performed with mitochondrial fractions prepared from wild-type and *SDH1-1/sdh1-1* 18-d-old seedlings. Heterozygous mutant plants consistently showed a 32% reduction in SQR activity (Fig. 1D). When 1 mM thenoyltrifluoroacetone, a known complex II inhibitor, was included in the assays, the activity was completely abolished. Thus, these heterozygous mutant plants have a mild reduction in complex II activity, a result consistent with their normal phenotype during sporophytic growth (see below).
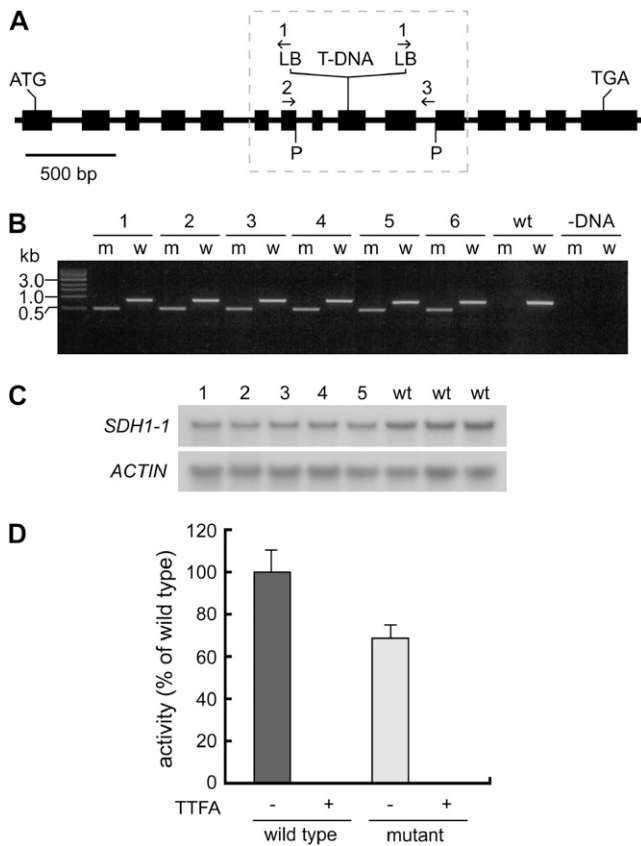
Figure 1. Identification of a mutant *sdh1-1* allele and molecular characterization of heterozygous mutant plants. A, Genomic organization of the *SDH1-1* gene. Exons are presented as black boxes. The T-DNA insertion site is indicated. Horizontal arrows show the position of primers. The T-DNA insert is not drawn to scale. LB, T-DNA left border; P, genomic *Pst*I sites flanking the T-DNA insert. B, Identification of heterozygous mutant plants. Genotyping was performed by PCR amplification with primers 1 and 2 to identify the mutant allele (m), and primers 2 and 3 to identify the wild-type allele (w). Six (1–6) heterozygous mutant plants were found. wt lanes correspond to a control with DNA from a wild-type plant, and lane −DNA to a PCR control without template. C, Northern-blot analysis of *SDH1-1* expression in five heterozygous mutant plants (lanes 1–5) and three wild-type plants (lanes wt). Each lane was loaded with 15 μg of total RNA isolated from flowers. The blot was hybridized with specific *SDH1-1* probe (derived from the 3′ UTR) and then with an actin probe as loading control. The *SDH1-1* transcript was present at a lower level in heterozygous mutant plants. D, Complex II activity is reduced in heterozygous mutant plants. SQR activity of wild-type and heterozygous mutant seedlings was determined in the presence or absence of thenoyltrifluoroacetone (TTFA), a complex II inhibitor. Three independent experiments were performed and the actual values were 17.8, 14.6, and 15.3 nmol of reduced DCIP min^{-1} mg^{-1} of protein for wild type seedlings, and 12.0, 10.5, and 10.1 nmol of reduced DCIP min^{-1} mg^{-1} of protein for mutant seedlings. Error bars correspond to SDs.

Since no other *sdh1-1* mutant alleles are available to establish a correlation between a phenotype (see below) and different mutations in *SDH1-1*, it was important to characterize the mutated *sdh1-1* locus and to analyze the number of T-DNA insertions in the mutant genome. PCR amplification of *SDH1-1* gene/T-DNA junctions first suggested that the insertion is complex. Indeed, both insertion sides were amplified using the left-border primer (primer 1 in Fig. 1A) in combination with either an upstream (primer 2) or a downstream (primer 3) gene-specific primer. Sequencing of the PCR products demonstrated that the T-DNA left border was present at both ends of the insertion, suggesting the presence of at least two T-DNA molecules. More importantly, sequence analysis established that no major deletions or chromosomal rearrangements took place during the insertional event. Only a minor 23 bp deletion occurred in *SDH1-1* at the insertion site.

T-DNA copy number was determined through DNA gel-blot analysis, using a T-DNA noncutting enzyme (*Pst*I). Hybridization of *Pst*I-restricted DNA with a T-DNA-specific probe identified two DNA fragments in the heterozygous mutant plants (Fig. 2, β-glucuronidase [GUS] probe). Although this result may suggest two independent insertions, all our attempts to segregate them apart, for instance, by backcrossing to wild-type plants, were unsuccessful. It is known that insertional events may be very complex and generate tandem arrays of T-DNA molecules in the same locus (De Neve et al., 1997; De Buck et al., 1999). To determine whether this occurred in our mutant, we sequentially hybridized the blot in Figure 2 with probes directed to the *SDH1-1* regions located upstream (probe 1) and downstream (probe 2) of the insertion (Fig. 2). Probe 1 (from a *Pst*I site in *SDH1-1* to the 5′ T-DNA insertion site) identified in the mutant DNA the 9 kb fragment also detected by the GUS probe, along with a 0.815 kb DNA fragment derived from the *SDH1-1* wild-type allele. Probe 2 (from the 3′ T-DNA insertion site to a *Pst*I site in *SDH1-1*) detected the other fragment (24 kb) identified by the GUS probe and the expected 0.815 kb DNA fragment of wild-type *SDH1-1*. These results are summarized in the scheme shown in Figure 2: both DNA fragments hybridizing to the T-DNA probe are derived from the *SDH1-1* locus, clearly showing that no other loci were interrupted by T-DNA insertions in the *SDH1-1/sdh1-1* heterozygous mutant plants. Therefore, Southern-blot analysis confirmed that these plants are heterozygous for the *sdh1-1* mutation and contained only one complex T-DNA insertion. It may be concluded that any phenotypic alteration will be due to the presence of the *sdh1-1* mutated allele.

Gametophytic Development Is Altered in *SDH1-1/sdh1-1* Heterozygous Mutant Plants

All the heterozygous *SDH1-1/sdh1-1* mutant plants were phenotypically indistinguishable from the wild type during vegetative development, at least under the growth conditions used. To examine flower development we used some parameters of the phenotypic analysis platform described by Boyes et al. (2001) for Arabidopsis. For instance, we did not find differences between heterozygous mutant and wild-type plants in flowering time, flower number and size, number and
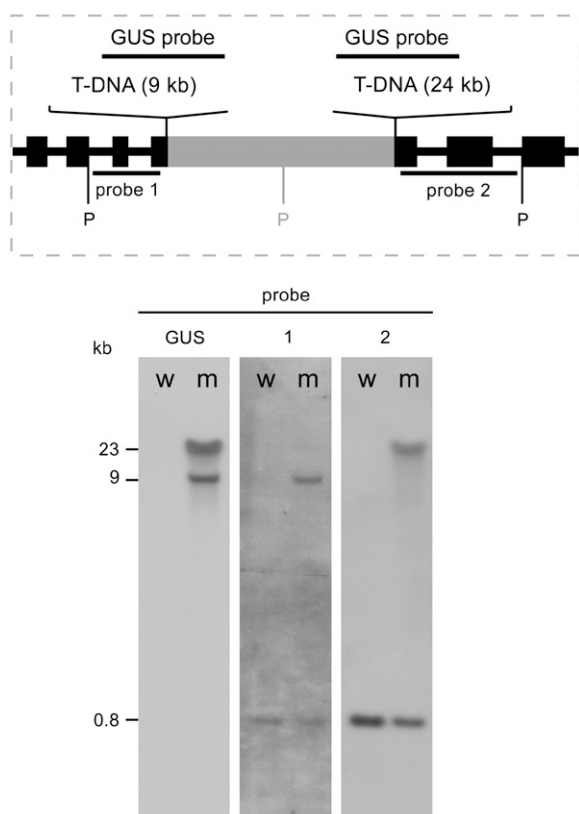
Figure 2. *SDH1-1/sdh1-1* plants contain a unique complex T-DNA insertion. Southern-blot analysis was performed to characterize the insertion. Total DNA (6 μg) from wt (w) or mutant (m) plants was digested with *PstI* and hybridized sequentially with probes directed to the T-DNA (GUS probe), the *SDH1-1* upstream region (probe 1), and the *SDH1-1* downstream region (probe 2). The presence of a new *PstI* restriction site (P) was inferred from the hybridization results and is shown in gray, in a sequence of unknown origin.

size of stamens, anther size, and anther dehiscence. However, microscopic analysis of mature pollen grains showed that significant numbers of abnormal and collapsed pollen grains were detected in the *SDH1-1/sdh1-1* mutant (Fig. 3B). Furthermore, *SDH1-1/sdh1-1* siliques contained a reduced seed set and were shorter than those of wild-type plants (Fig. 3C). Closer examination of *SDH1-1/sdh1-1* siliques revealed the presence of small, white, unfertilized ovules (Fig. 3D). No seed of an intermediate size indicative of abortion after fertilization was observed. Seed set per silique was quantitatively determined, using six T_3 *SDH1-1/sdh1-1* plants and two wild-type plants grown hydroponically in the same batch. The average seed set per silique was reduced by 33% in the *SDH1-1/sdh1-1* mutant plants (last bars, Fig. 3E), suggesting that only 67% of the ovules were fertilized in these plants. Moreover, reduction of seed production in mutant plants was evenly distributed along the inflorescence axis, indicating that the overall seed set reduction in the mutant is not due to the presence of flowers not producing seeds along with flowers giving a normal seed number (Fig. 3E).

Altogether, these observations suggest that both pollen and embryo sac development are compromised in the heterozygous *SDH1-1/sdh1-1* mutant plants, and that the *sdh1-1* mutation is gametophytic (Park et al., 1998; Drews and Yadegari, 2002; Johnson-Brousseau and McCormick, 2004; Niewiadomski et al., 2005). Indeed, the presence of abnormal pollen (along with normal pollen) would not be sufficient to explain a reduced seed set, since pollen is supposed to be in great excess with respect to ovules.

Genetic Analysis of the Mutated *sdh1-1* Allele

The T-DNA insertion in the *SDH1-1/sdh1-1* mutant plants confers kanamycin resistance (Kan[r]). Segregation of Kan[r] was analyzed in the progeny of six selfed T_2 heterozygous *SDH1-1/sdh1-1* plants (Supplemental Table S1). From a total of 1,243 offspring, only 387 seedlings were kanamycin resistant. This segregation ratio of 0.5:1 for Kan[r]:Kan[s] (kanamycin sensitive) is far below from the expected 3:1 segregation for a dominant resistant phenotype and from the 1:1 expected ratio for a fully penetrant mutation in either the male or female gametophyte, and is indicative of a gametophytic defect affecting both the male and female parents (Howden et al., 1998). To test this, male and female transmission efficiencies (TEs) of the mutated *sdh1-1* allele were determined by performing reciprocal test crosses between the heterozygous *SDH1-1/sdh1-1* mutant and wild-type plants (Park et al., 1998). The F_1 progenies were genotyped by PCR and analyzed for Kan[r] or sensitivity (Supplemental Table S2). As expected, all Kan[r] seedlings carried the *sdh1-1* mutated allele along with the *SDH1-1* wild-type allele, and all Kan[s] plants only bore the wild-type allele. When the heterozygous *SDH1-1/sdh1-1* mutant was used as the male parent, no seedlings bearing the mutated *sdh1-1* allele were found (male TE of 0%). When the heterozygous mutant was used as the female parent, a female TE of 60% was measured (33 instead of 55 seedlings bearing the mutated allele). Thus, the observed segregation ratio of 0.5:1 in selfed heterozygous plants was caused by defects in both male and female gametophytes, resulting in reduced TE of the mutated allele. Altogether, these results showed that all the pollen grains and about half the ovules bearing the mutated *sdh1-1* allele were unable to transmit this allele.

Therefore, the *sdh1-1* mutation is partially penetrant in the female gametophyte and fully penetrant in the male gametophyte, strongly suggesting that complex II activity is essential for pollen development and important for embryo sac development.

Pollen Development Is Perturbed in *SDH1-1/sdh1-1* Mutant Plants

Our genetic analyses demonstrated that the male germ line was unable to transmit the *sdh1-1* mutated allele and prompted us to analyze pollen development
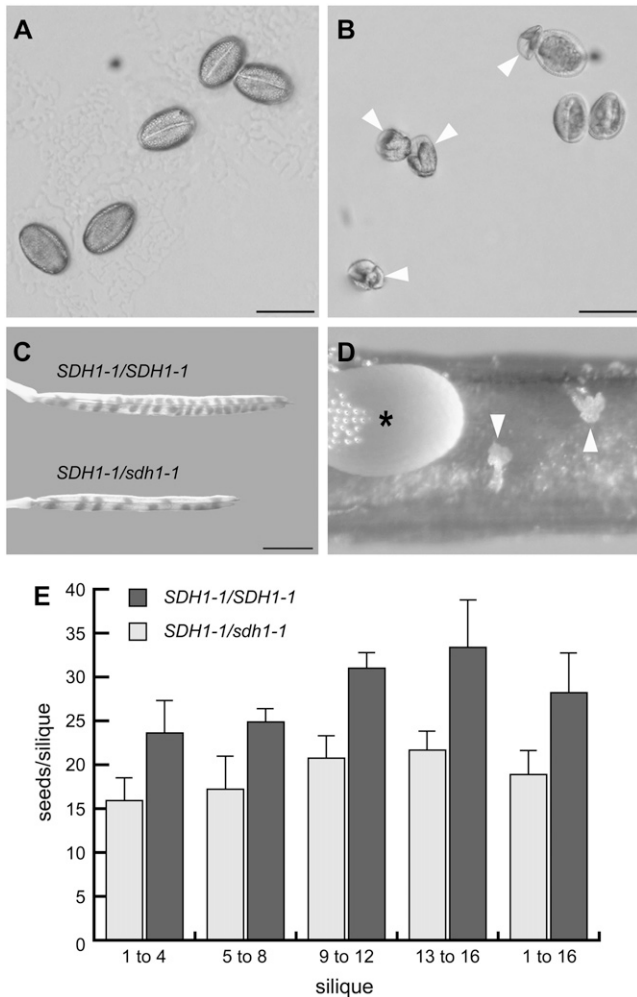
Figure 3. Reproductive abnormalities in *SDH1-1/sdh1-1* mutant plants. A, Mature pollen grains from a wild-type plant. Bar = 20 µm. B, Mature pollen grains from a heterozygous mutant plant. A substantial proportion of pollen grains are collapsed (arrowheads). Bar = 20 µm. C, Mature siliques of a *SDH1-1/sdh1-1* plant are shorter and contain less seeds than mature siliques of the wild type. Bar = 2 mm. D, Closeup of a developing *SDH1-1/sdh1-1* silique. Arrowheads denote aborted, white, and shrunken ovules. A wild-type seed is indicated by an asterisk. E, Seed set is reduced in *SDH1-1/sdh1-1* siliques. Seed set per silique was scored along the main inflorescence axis for six T₃ Kanʳ *SDH1-1/sdh1-1* plants and two wild-type plants. Silique 1 (first, older flower) to silique 16 were grouped in four groups of four siliques for each plant. Total counts of 28.2 and 18.9 seeds/silique were obtained for wild type and *SDH1-1/sdh1-1* plants, respectively (last two bars). Error bars are SDs.

in detail. First, pollen of wild-type and *SDH1-1/sdh1-1* plants was analyzed for viability by the staining method of Alexander (1969). In this assay, mature viable pollen grains show an intensive purple stain in the cytoplasm, surrounded by a thin green stain of the external exine layer (Fig. 4, A and C). In the *SDH1-1/sdh1-1* mutant, mature viable pollen grains were found (Fig. 4B). However, aborted pollen grains showing only the green staining of the external exine layer were abundant (Fig. 4, B and D). To determine the frequency

of dead pollen in the *SDH1-1/sdh1-1* mutant, pollen from 12 heterozygous T₃ mutant plants was stained with Alexander's solution. Nonviable pollen grains occurred with a frequency of 41.6% to 49.4% (Supplemental Table S3). From a total of 3,133 pollen grains, 1,448 (46.2%) were not viable according to the Alexander staining test. Thus, these figures show low variability of the pollen phenotype among different plants and are consistent with the genetic data in the sense that near half of the pollen grains, those carrying the mutated *sdh1-1* allele are not viable.

Second, we compared anther and pollen development in *SDH1-1/sdh1-1* and wild-type plants (Fig. 5). Anther development has been divided into 14 stages based on morphological landmarks and cellular events visible under the light microscope (Sanders et al., 1999). Anthers of the *SDH1-1/sdh1-1* mutant were indistinguishable from those of wild type at stage 9 (Fig. 5, A and B). At this stage, meiosis has already been completed, the exine wall is deposited on microspore surface, microspores contain a large vacuole, and the microspore nucleus is located at the cell periphery. Anthers of the mutant deviated from wild type at stage 11, when pollen mitotic divisions and vacuole resorption occur (Fig. 5, C and D). Besides normal pollen grains, which have both vegetative and generative nuclei, a dense cytoplasm, and small vacuoles, abnormal pollen grains were clearly visible. In these altered pollen grains, mitosis did not occur and
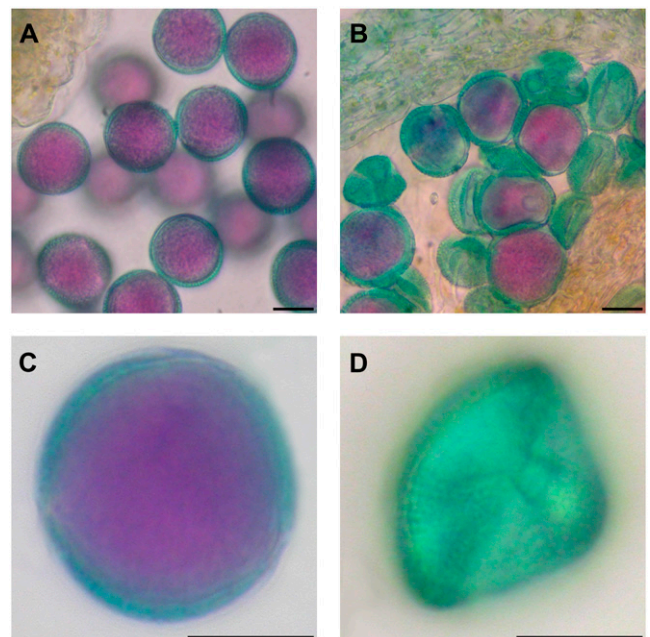

Figure 4. Loss of *SDH1* function affects pollen viability. Alexander's staining was performed with wild type (A and C) and heterozygous *SDH1-1/sdh1-1* mutant (B and D) anthers. In these bright-field images, wild-type, viable pollen grains show intensive purple staining in the cytoplasm, whereas dead, unviable pollen grains are devoid of cytoplasm and exhibit only the green staining of the exine outer layer. Bars = 10 µm.

the vacuole persisted. Moreover, the cytoplasm detached from the external exine layer and was progressively degraded (compare early stage 11 in Fig. 5C with late stage 11 in Fig. 5D). At stage 12, just prior to dehiscence, the abnormal pollen grains showed varying degrees of damage, including some in which the cellular material disappeared and the exine layer collapsed (Fig. 5E). It has to be pointed out that mutant *SDH1-1/sdh1-1* anthers were not detectably different from those of wild-type plants, except for these described pollen abnormalities. For instance, other anther tissues like the epidermis, endothecium, and vascular bundle were not affected. Furthermore, mutant and wild-type anthers underwent the same events at similar stages, including disappearance of the tapetum and normal dehiscence.

Transmission electron microscopy was conducted on cross sections of wild-type and mutant *SDH1-1/sdh1-1* anthers (Fig. 6). By the vacuolated microspore stage, mutant microspores were not detectably different from those of wild-type plants (Fig. 6, A and B; Owen and Makaroff, 1995). Numerous mitochondria and starch-containing plastids are present throughout the cytoplasm, the exine is essentially complete and just below it vesicles produced by the microspores add material to the intine. While the nucleus is located near the side of the microspore, the asymmetric first mitotic division occurs, producing bicellular pollen grains (Fig. 6C). The generative cell is located at one end of the pollen grain and is surrounded by a wall that is continuous with the intine. At this stage, however, the *SDH1-1* defect was evident in pollen sacs of *SDH1-1/sdh1-1* anthers, since a mixture of wild-type-like (Fig. 6C) and altered microspores (Fig. 6D) were found within the locule. Abnormal pollen grains never underwent microspore mitosis, the large vacuole persisted, and the plasma membrane was withdrawn from the cell wall.

In *SDH1-1/sdh1-1* anthers, wild-type-like pollen grains followed a normal developmental fate: generative cell occupies a more central location in the cytoplasm of the vegetative cell, the large vacuole is resorbed (Fig. 6E), and lipid bodies accumulate in the vegetative cells at the surface of the generative cell (Fig. 6F). Later, the cytoplasm of the vegetative cell becomes highly vacuolated (Fig. 6G). Neither of these landmarks of normal pollen development was observed in altered pollen grains. In these grains, autolysis led to the disintegration of cellular structures and progressive disappearance of cellular content (Fig. 6, H and I). Finally, pollen grains had collapsed completely (Fig. 6J).

Embryo Sac Development Is Defective in *SDH1-1/sdh1-1* Mutant Plants

Reduced seed set, accompanied by the presence of white, small senescing ovules, and reduced transmission of the *sdh1-1* mutation through the female gametophyte, suggested defects in embryo sac maturation

and led us to analyze the phenotype of female gametophytes. To do this, we allowed the female gametophytes within wild-type and heterozygous pistils to progress to the terminal developmental stage, in the absence of fertilization, and embryo sacs were examined under Nomarski optics. In ovaries of wild-type plants, all embryo sacs reached the terminal developmental stage, containing one secondary central cell nucleus, one egg cell nucleus, and two synergid cell nuclei (Fig. 7A). In mutant plants, only 72.75% ($n = 291$) of embryo sacs displayed the wild-type phenotype (Fig. 7B). In addition, two abnormal phenotypes were observed. In 14.75% ($n = 59$) of the analyzed ovules, embryo sacs were arrested at the two-nucleate stage (Fig. 7C), and in 12.5% of the embryo sacs ($n = 50$) the overall morphology of the egg cell, central cell, and synergid cells was normal, yet polar nuclei failed to fuse (Fig. 7D). Therefore, 27% of the embryo sacs in *SDH1-1/sdh1-1* plants were phenotypically mutant, a value in good agreement with the seed set reduction (33%).

Down-Regulation of *SDH1-1* by RNA Interference Results in a Phenotype Similar to That of the Insertional Mutant

Since no other mutant alleles were available for *SDH1-1*, an RNA interference approach was used. Figure 8A illustrates the construct: the 35S RNA promoter of the *Cauliflower mosaic virus* drives the transcription of partial *SDH1-1* sequences cloned in sense and antisense orientations and separated by a plant intron. After formation of hairpin RNA structures (ihpRNA) and splicing, the resulting double-stranded RNA transcripts can cause posttranscriptional silencing of endogenous gene activity (Smith et al., 2000). After floral-dipping transformation, only two independent transgenic T_1 plants were obtained. Since mature gametophytes or recently fertilized embryos are the likely targets of this transformation procedure (Clough and Bent, 1998), this low efficiency of transformation is consistent with our results showing that gametophyte development is affected in the *SDH1-1/sdh1-1* mutant. Moreover, northern-blot analysis of these primary transformants showed that *SDH1-1* mRNA levels are only partially reduced (roughly 50%, data not shown), suggesting that a drastic reduction in *SDH1-1* expression may lead to unviable transformed embryos.

T_2 seeds from one of these two lines were germinated on kanamycin and five resistant seedlings were transferred to hydroponic medium. Northern-blot analysis was performed using RNA from these five transgenic plants and two wild-type plants. The results are shown in Figure 8B, with actin as a constitutive control. Compared to wild-type plants, all transgenic plants showed a decrease in the *SDH1-1* mRNA levels. These RNAi plants were phenotypically indistinguishable from the wild type during sporophytic development. However, analysis of pollen
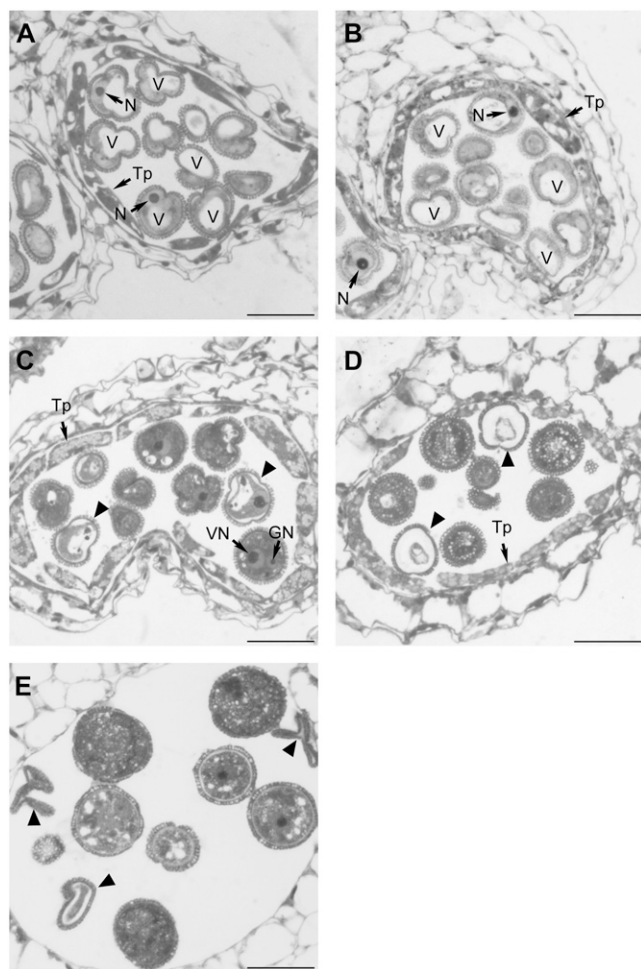
Figure 5. Pollen development in *SDH1-1/sdh1-1* mutant plants. Anther sections were stained with Toluidine blue and photographed by bright-field microscopy. Abnormal pollen grains are indicated by arrowheads. Magnification is the same in all micrographs (Bars = 20 μm). GN, Generative cell nucleus; N, nucleus; Tp, tapetum; V, vacuole; VN, vegetative cell nucleus. A, Anther from the wild type at the vacuolated microspore stage. B, Anther from the *SDH1-1/sdh1-1* mutant, at the vacuolated microspore stage. All microspores are indistinguishable from those of wild-type anthers. C, Anther from the *SDH1-1/sdh1-1* mutant after pollen mitosis I, showing normal pollen grains with two nuclei, and abnormal pollen grains (arrowheads) not entering mitosis. D, Anther from the *SDH1-1/sdh1-1* mutant after pollen mitosis II, showing normal pollen grains with a dense cytoplasm, and abnormal pollen grains (arrowheads) containing cell debris. E, Anther just before dehiscence, containing mature pollen grains and collapsed pollen grains devoid of cytoplasm (arrowheads).

viability by the staining method of Alexander showed varying percentages, ranging from 13.5% to 66.8% of dead, unviable pollen grains (Fig. 8, C and D). Moreover, seed set was significantly reduced in the transgenic plants bearing the RNAi construct (Fig. 8E). Interestingly, a correlation was found between the level of *SDH1-1* mRNA expression and the degree of seed set reduction and pollen abortion (for instance, plant no. 5 showed the strongest reduction in mRNA, pollen viability, and seed set).

In conclusion, plants in which *SDH1-1* gene expression is decreased by dsRNA showed the same phenotype as the heterozygous insertional mutant plants, i.e. reduced seed set and pollen abortion.

DISCUSSION

SDH1 genes are interesting targets for reverse genetics analysis, to gain insights into the role of complex II in plants. Thus, we have characterized knockout alleles of *SDH1-1* and *SDH1-2* genes. The *SDH1-2* gene appears to be dispensable, at least under the growth conditions used, presumably because the *SDH1-1* gene encodes the predominant flavoprotein. Our results do not rule out a *SDH1-2* nonessential role in a restricted group of cells or in a particular developmental stage, resulting in subtle beneficial characteristics. Such a hypothesis may provide an explanation for *SDH1-2* integrity and conservation when compared to *SDH1-1*. Alternatively, *SDH1* duplication may be very recent, evolutionarily speaking, and either *SDH1-2* inactivation or *SDH1-2* gain of a new function are under way.

Molecular and genetic characterization of heterozygous *SDH1-1/sdh1-1* mutant plants permit us to conclude that *sdh1-1* is a gametophytic mutation affecting both male and female gametophyte development. *SDH1-1* is essential for pollen development and the first defect was evident in *sdh1-1* microspores at pollen mitosis I, the asymmetric mitosis that results in bicellular pollen grains. Mutant microspores never underwent mitosis, the large vacuole was not resorbed, and cellular content progressively disappeared. These results formally established that microspore mitochondria (and complex II) have an essential role in pollen development.

During male gametophyte development, defined as development of the haploid microspores, pollen grains show a very high metabolic activity. For instance, respiration rates are 10 times higher in pollen grains than in green tissues (Tadege and Kuhlemeier, 1997). The uninucleate microspore develops to trinucleate pollen through two mitotic divisions, and simultaneously starch, proteins, and other nutrients enrich the pollen of the vegetative cell (McCormick, 2004). These processes put demands on energetic and metabolic resources for the synthesis of proteins and other biomolecules. In Arabidopsis, all the genes for complex II components, with the exception of *SDH1-2* and *SDH2-3*, show enhanced expression in floral tissues (Figueroa et al., 2001, 2002). Furthermore, digital northern analysis of developing pollen grains (Honys and Twell, 2004) shows that these genes are expressed in the male gametophyte (Supplemental Fig. S2). Considering that SDH is a component of the respiratory chain and the TCA cycle, loss of SDH1 in microspores would severely compromise both ATP production and provision of carbon skeletons for biosynthesis, leading to their abortion.

In addition to its essential role during pollen development, *SDH1-1* is important for normal embryo sac
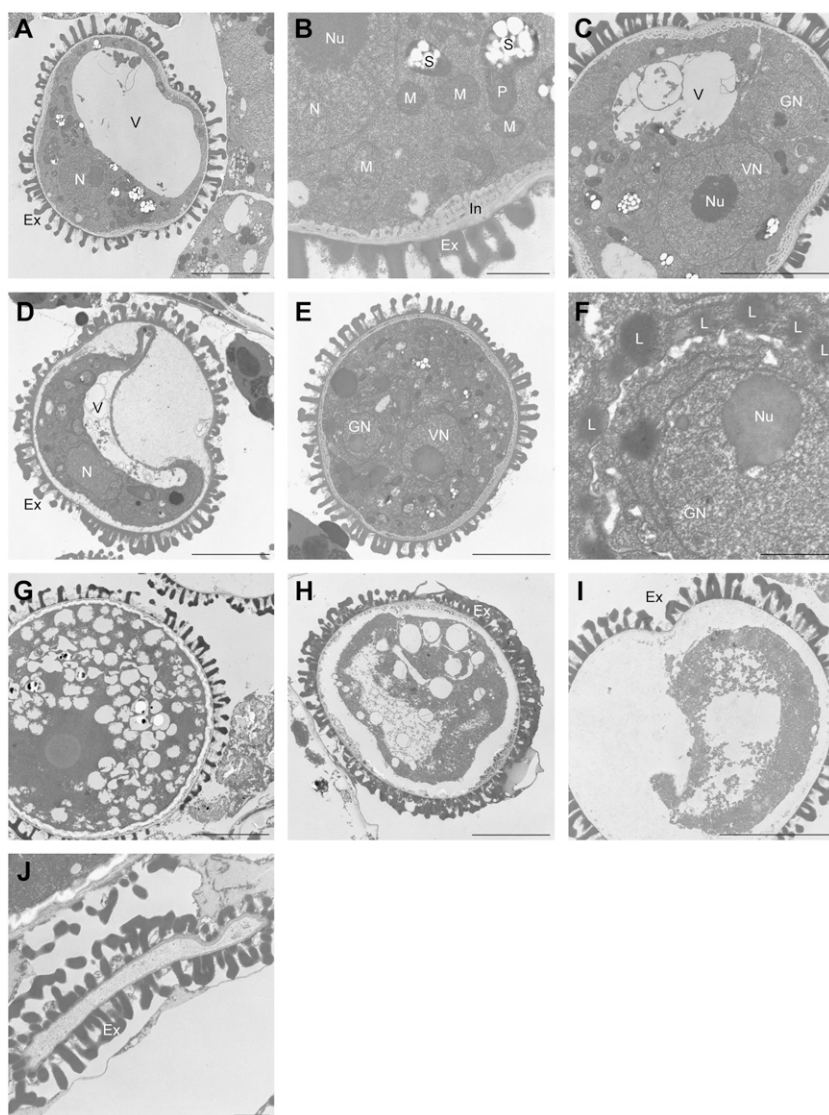
Figure 6. Transmission electron microscopy analysis of anthers in the *SDH1-1/sdh1-1* mutant. Ex, Exine layer; GN, generative nucleus; L, lipid body; M, mitochondrion; N, nucleus; Nu, nucleolus; S, starch granules within plastids; V, vacuole; VN, vegetative nucleus. Bar = 5 μm in A, C to E, and G to I; bar = 1 μm in B, F, and J. A, Microspores at the vacuolated stage (anther stage 9 according to Sanders et al., 1999). All microspores had wild-type morphology, with numerous mitochondria, starch granules within plastids, and a normal exine outer layer. B, Closeup of the microspore shown in A. C, Bicellular pollen grain from *SDH1-1/sdh1-1* anthers. The asymmetric first mitotic division has occurred (early anther stage 11). D, Same anther as in C. In addition to pollen with wild-type morphology (C), abnormal pollen grains were present. They did not undergo mitosis and cell content detached from the outer layers. E and F, Later developmental stage of wild-type pollen grains from *SDH1-1/sdh1-1* anthers. G, Mature wild-type pollen grain from *SDH1-1/sdh1-1* anthers. H and I, Later developmental stages of aberrant pollen grains from *SDH1-1/sdh1-1* anthers. Cellular structures and content progressively disappeared and internal structures were no longer distinguishable. J, Collapsed pollen grain in the same anther as in G. The exine layer, of sporophytic origin, remained wild-type like.

development. Although our data indicate that the SDH1-1 protein is essential for efficient megagametophyte development, a fraction of the gametophytes still remains functional. Therefore, these mutant gametophytes cannot be completely energy deficient. The more plausible explanations for this observation are (1) a stochastic inheritance and persistence of wild-type mitochondria from the diploid megaspore mother cell, which would result in variable depletion rates of SDH1-1 through cell division and protein turnover during embryo sac development, and/or (2) variable provision of nutrients (ATP, carbon skeletons) to the female gametophyte from the surrounding sporophytic cells. In this context, it is tempting to speculate that male mutant gametophytes have a more severe phenotype because more nutrients are carried from sporophytic tissues to the female than to the male gametophyte. These arguments may also explain why more than one phenotype was found in the mutant embryo sacs (see below).

During megagametogenesis, a functional haploid megaspore gives rise to the mature female gametophyte (Yadegari and Drews, 2004). This process comprises three successive rounds of nuclear division, followed by cellularization. During cellularization, the two polar nuclei migrate to the center of the female gametophyte and fused together in the central cell. The result is a seven-cell embryo sac that contains three antipodal, two synergid, one egg, and one central cell. Two abnormal phenotypes were observed in *sdh1-1* embryo sacs, developmental arrest at the two-nucleate stage, and failure of the two polar nuclei to fuse after their proper migration.

Large collections of gametophytic mutants defective in female gametophyte development have been reported, and in some cases characterized with respect to the genes responsible for the observed defects (e.g. Christensen et al., 2002; Yadegari and Drews, 2004; Niewiadomski et al., 2005; Pagnussat et al., 2005; Portereiko et al., 2006). A wide variety of phenotypes
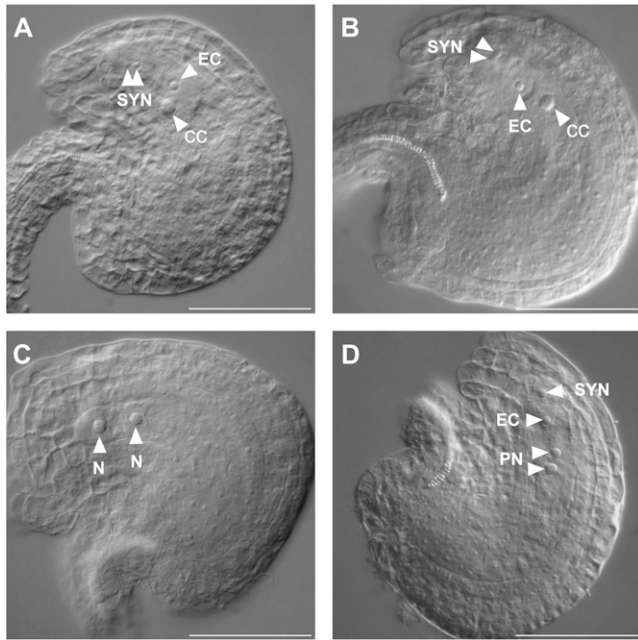
Figure 7. Embryo sac development defects in *SDH1-1/sdh1-1* mutant plants. Flowers of wild-type and *SDH1-1/sdh1-1* plants were emasculated, and whole-mount preparations of ovules were analyzed by DIC microscopy 48 h after emasculation. Embryo sac nuclei are indicated by arrows. A, Ovule from a wild-type Ws plant. The embryo sac is at the terminal developmental stage and contains one secondary nucleus in the central cell, one egg cell nucleus, and two synergid cell nuclei at the micropylar end. B, Ovule harboring a wild-type-like embryo sac in a *SDH1-1/sdh1-1* mutant plant. C, Ovule from the same pistil of the ovule shown in B. The embryo sac displays a mutant phenotype, being arrested at the two-nucleate stage. D, Ovule from the same pistil of the ovule shown in B and C, but showing a second mutant phenotype. The two polar nuclei lie side by side but failed to fuse. CC, Central cell nucleus; EC, egg cell nucleus; N, nuclei from an embryo sac arrested at the two-nucleate stage; PN, polar nuclei; SYN, synergid cell nuclei. Bars = 50 μm.

were observed, including mutants arrested at the two-nucleate stage and mutants cellularized but with defects in fusion of the polar nuclei. Interestingly, among the mutants affected in fusion of polar nuclei, several of the mutated genes encode mitochondrial proteins or predicted mitochondrial proteins (Christensen et al., 2002; Portereiko et al., 2006). The best characterized are GFA2, a mitochondrial matrix chaperone of the DnaJ protein family (Christensen et al., 2002), RPL21M, a mitochondrial 50S ribosomal subunit L21 (Portereiko et al., 2006), and now SDH1-1 (this work). Altogether these results strongly suggest a role for mitochondria in nuclear fusion (karyogamy). At this time, it is unclear why these mutants have a nuclear fusion defect. However, the fact that mutations in a ribosomal protein, a chaperone, and a complex II subunit lead to a similar phenotype favors the hypothesis that the karyogamy defect is a consequence of impairment in basic mitochondrial functions, like electron transport, ATP production, and/or provision of carbon skeletons.

Few defects in the respiratory chain and TCA cycle have been reported. For instance, a knockout mutation

in a subunit of the NAD^+-dependent isocitrate dehydrogenase has been described in Arabidopsis (Lin et al., 2004). The homozygous mutant plants showed no detectable differences in vegetative growth and reproductive development compared to wild-type plants. However, Arabidopsis contains multiple genes
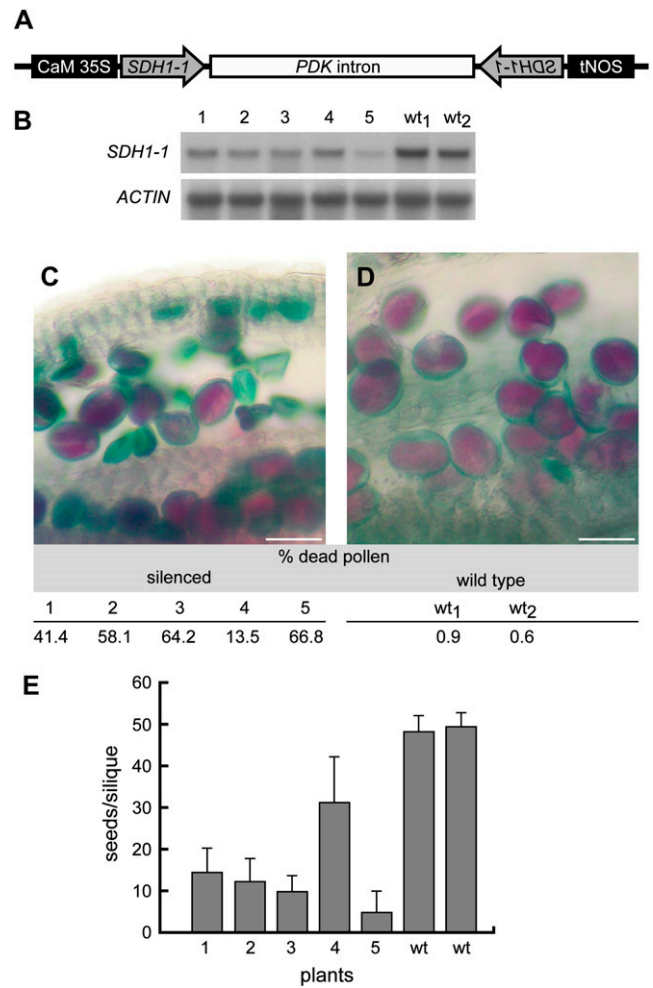

Figure 8. Phenotype of *SDH1-1* RNAi transgenic plants. A, Schematic diagram of the construct used to down-regulate *SDH1-1*. The arrows indicate the *SDH1-1* sequence (first exon) cloned in both orientations in the RNAi pHELLSGATE4 vector. Sense and antisense *SDH1-1* transcribed sequences would be separated by the plant pyruvate orthophosphate dikinase (PDK) intron, generating an ihpRNA. B, Northern-blot analysis of *SDH1-1* expression in five RNAi T_2 plants and two wild-type controls. Each lane was loaded with 10 μg of total RNA isolated from flowers. The blot was hybridized with a *SDH1-1* specific probe and then with an actin probe as loading control. RNAi plants had decreased *SDH1-1* mRNA levels. C and D, Pollen abortion in *SDH1-1* RNAi plants. Alexander staining was performed on two wild-type and five RNAi T_2 anthers. Sections C and D show the staining of one RNAi plant and one wild-type plant, respectively. Quantitative determination of pollen abortion was done by counting viable, purple pollen grains, and aborted, green pollen grains, and the results obtained are shown under the images. Bars = 20 μm. E, Seed set is reduced in *SDH1-1* RNAi plants. Seed set per silique was scored for the first eight siliques from five T_2 RNAi plants (1–5) and two wild-type control plants (wt). Error bars represent SDs.

encoding catalytic and noncatalytic subunits of this enzyme, and in mitochondrial extracts from homozygous mutant plants there was still half as much enzyme activity as in wild-type plants. Antisense repression of the potato (*Solanum tuberosum*) mitochondrial citrate synthase gene resulted in a delaying flowering phenotype and a specific disintegration of the ovary tissues, indicating an important role of the TCA cycle during the early stages of flower development and the formation of the sporophytic female tissues (Landschütze et al., 1995). Additional efforts to analyze the function of the TCA cycle have been performed in a mutant (*Aco1*) that exhibits a deficiency in expression of one of two isoforms of aconitase present in tomato (*Lycopersicon esculentum*; Carrari et al., 2003), and in antisense transgenic plants exhibiting reduced activity of mitochondrial malate dehydrogenase (Nunes-Nesi et al., 2005). However, the possible presence of multiple genes has not been analyzed, these plants still maintain mitochondrial aconitase and malate dehydrogenase activities, and their reproductive development is not affected.

The best-characterized respiratory chain mutant is a *Nicotiana sylvestris* mitochondrial mutant, CMS II. In this mutant, the mitochondrial *nad7* gene encoding the NAD7 subunit of complex I is deleted, and mitochondria are impaired in complex I structure and function (Pla et al., 1995; Gutierres et al., 1997). The absence of a competent complex I leads to impaired photosynthesis and slower growth, however plants attain biomass similar to that of wild-type plants and undergo reproductive development, although they are partially male sterile (Gutierres et al., 1997; Dutilleul et al., 2003a). Therefore, mutant plants were acclimated to this defect and this acclimation includes enhanced activity of nonphosphorylating NAD(P)H dehydrogenases, which bypass complex I (Sabar et al., 2000; Dutilleul et al., 2003a, 2003b). An Arabidopsis mutant lacking the 18 kD Fe-S subunit of complex I has also been described and shown to be affected in cold acclimation (Lee et al., 2002). Homozygous mutant plants grow more slowly than wild-type plants and a delay was observed in flowering. Nevertheless, these plants eventually reach heights similar to those of wild-type plants and were fully fertile. Altogether, data with these mutants indicate that a defect in complex I in plants is not lethal. In contrast, loss of complex II leads to a more severe phenotype, at least in gametophytic development, and this is probably due to the role of SDH in the TCA cycle.

Deficiencies of any of the four subunits of SDH are associated with a broad spectrum of human diseases, ranging from myo- and encephalopathies to aging and tumor formation (Rustin and Rötig, 2002). To our knowledge, the first reported nuclear gene mutation causing a respiratory chain defect in humans was a mutation in the gene encoding the complex II flavoprotein subunit (Bourgeron et al., 1995). The mutation was identified in two siblings presenting Leigh syndrome (necrosis of specific brain territories, causing

encephalopathy) and SDH deficiency, and the patients were homozygous for an amino acid substitution in a conserved domain of the protein. It has to be emphasized that the available data suggest that complex II is essential in mammals and could not be completely lost. For instance, Piruat et al. (2004) reported the generation of a SDH4 knockout mouse, the first mammalian model lacking a protein of the mitochondrial electron transport chain, and showed that homozygous *sdh4/sdh4* animals die at early embryonic stages.

Although development and function of gametophytes are crucial for plant reproduction, relatively little is known about the genes required for, and the pathways involved in gametophytic development in flowering plants. An important question is whether plants exploit metabolism as a way to control development. We have found here that an apparent metabolic mutant shows developmental effects, raising the possibility that some developmental regulators exert their effects through the modulation of basic metabolic processes. Metabolic regulation thus should be considered as one possible effector pathway in models of genetic regulation of development.

MATERIALS AND METHODS

Plant Material and Growth Conditions

Arabidopsis (*Arabidopsis thaliana*) ecotype Wassilewskija (Ws) seeds were cold treated for 48 h at 4°C in darkness and then germinated and grown hydroponically at 20°C to 24°C, under a 16-h light/8-h dark cycle (Gibeaut et al., 1997). To grow seedlings in vitro and for Kan^r assays, seeds were surface sterilized for 10 min with a solution of 10% (v/v) commercial bleach and 0.05% (v/v) Tween 20. Then seeds were rinsed thoroughly with sterile distilled water and sown on one-half-concentrated Murashige and Skoog medium solidified with 0.8% (w/v) agar and supplemented or not with 50 mg L^{-1} kanamycin. Finally seeds were cold treated, germinated, and grown as described above.

Isolation of Insertional *SDH1* Mutants

The Arabidopsis Knockout Facility (AKF) alpha and BASTA populations (Sussman et al., 2000) were screened by PCR, using a primer specific for the T-DNA left border (JL 202, 5′ CATTTTATAATAACGCTGCGGACATCTAC 3′) in combination with either a forward or a reverse gene-specific primer. For *SDH1-1*, the forward primer was 5′ GGAGTGAGAATAGGGGTAATTAAGGGAAT 3′ and the reverse primer was 5′ CTGGAGTAAAACGTAAACCCAGTTTCAGA 3′. For *SDH1-2*, forward and reverse primers were 5′ TATTTCACTGCTGCAACATTATGGGCTTT 3′ and 5′ GATGGACGGTCTCGATTAAACGGTTAGAT 3′, respectively. Identification of DNA positive pools was performed by DNA gel-blot analysis of the PCR products, using *SDH1-1* or *SDH1-2* gene fragments as probes, and confirmed by sequencing of the amplified DNA (see Sussman et al., 2000 and http://www.biotech.wisc.edu/NewServicesAndResearch/Arabidopsis/OverviewIndex.html for methods). Only one insertion in each *SDH1-1* and *SDH1-2* were found (both in the AKF alpha mutant collection).

The Salk Institute collection (Alonso et al., 2003), the Torrey Mesa Research Institute collection (Sessions et al., 2002), and the Wisconsin DsLox T-DNA lines (http://www.hort.wisc.edu/krysan/DS-Lox) were searched in silico at two sites: the Arabidopsis Insertion Database (http://atidb.org/cgi-perl/index) and the T-DNAExpress Web sites (http://signal.salk.edu/cgi-bin/tdnaexpress). Although several mutant alleles were identified for *SDH1-2* (e.g. SALK_015173 and SALK_087371), no T-DNA additional insertions were found in the *SDH1-1* gene. A line in the Wisconsin DsLox T-DNA population (DsLox501H11) indexed as a *SDH1-1* mutant was further characterized and found to carry the T-DNA insertion downstream of the *SDH1-1* 3′ untranslated region (UTR; data not shown).

Arabidopsis Ws seeds from the positive AKF pools containing the *sdh1-1* and *sdh1-2* mutant alleles were obtained from the ABRC (Ohio State University, Columbus, OH). These T_2 seeds were stratified, germinated, and grown as described above. To identify *SDH1* mutant plants and eventually isolate plants homozygous for a mutation, seedlings were genotyped by a PCR-based approach, using total DNA extracted from one cotyledon or one small leaf. Briefly, tissue was homogenized in 100 μL of TNE/SDS buffer (0.2 M Tris-HCl pH 8.0, 0.25 M NaCl, 0.02 M EDTA, 0.5% [w/v] SDS), using a disposable pestle adapted to a portable drill. After a 5 min centrifugation at 14,000g, the DNA in the supernatant was precipitated with 1 volume of isopropanol, washed with 70% (v/v) ethanol, and resuspended in sterile water. The genotype of plants was determined by PCR using primers flanking the insertion point for the wild-type allele and a gene-specific and left border-specific (JL202) primer pair for the insertional mutant alleles. For *SDH1-1*, the wild-type allele was amplified with 5' CAACCTCAGCACATACATGCACAG 3' (primer 2 in Fig. 1A) and 5' CCATCTCATGCTTAACTCCACACA 3' (primer 3 in Fig. 1A), and the mutant allele with JL202 (primer 1 in Fig. 1A) and primer 2. For *SDH1-2*, the wild-type allele was amplified with 5' TATTTCACTGCTGCAACATT-ATGGGCTTT 3' (primer sdha3) and 5' GATGGACGGTCTCGATTAAACG-GTTAGAT 3' (primer sdha4), and the mutant allele with JL202 and sdha4.

Nucleic Acids Preparation and Analysis

Total DNA was prepared from green leaves according to Ausubel et al. (1994). Total RNA was isolated from tissues harvested into liquid nitrogen using TRIzol reagent and the manufacturer's protocol (Invitrogen). Southern and northern analyses were performed by standard procedures with ^{32}P-labeled probes (Ausubel et al., 1994). To obtain specific probes, DNA fragments were PCR amplified using the following primer pairs: for a T-DNA GUS probe (Fig. 2), 5' TCTACACCACGCCGAACACCTGG 3' and 5' TTC-GGTGATGATAATCGGCTGATGC 3'; for probe 1 in Figure 2, 5' CTGCA-GGTTTTCCACCTGTTTC 3' and 5' ACGTTCACCTTCACTGTTTCTA 3'; for probe 2 in Figure 2, 5' AACGATATGCTCCTACAGCCAA 3' and 5' CCATCT-CATGCTTAACTCCACACA 3'; for a *SDH1-1* probe derived from the 3' UTR, 5' TGAGATTGGATTATAGGCCTGTT 3' and 5' CTGGAGTAAAACGTAA-ACCCAGTTTCAGA 3'; and for an actin probe, 5' GCTATGTATGTCGC-CATTCAAGC 3' and 5' CATCATATTCTGCCTTTGC(A/G)ATCC 3'.

Preparation of Mitochondria and SQR Activity Assay

A crude mitochondrial fraction was prepared from Arabidopsis in vitro-grown 18-d-old seedlings. All steps were performed at 2°C to 4°C. The tissue (1 g fresh weight) was chilled in 10 mL of ice-cold grinding buffer (0.03 M MOPS/KOH pH 7.5, 0.3 M Mannitol, 0.001 M EDTA, 0.004 M L-Cysteine, 0.1% [w/v] fatty acid-free bovine serum albumin [fraction V], 0.6% [w/v] Poly-vinylpyrrolidone-40) and homogenized with a Dounce potter. The homogenate was filtered through Miracloth and the filtrate was centrifuged at 1,000g for 20 min. The supernatant was then centrifuged at 12,500g for 20 min and the pellet was suspended in washing buffer (0.03 M MOPS/KOH pH 7.5, 0.3 M Mannitol, 0.001 M EDTA). Both centrifugation steps were repeated. Finally, the pellet (crude mitochondrial fraction) was resuspended in 200 μL of washing buffer. Protein concentration was determined by the Bradford method (Bradford, 1976) and SQR activity assayed immediately.

SQR activity was determined as described by Miyadera et al. (2003). Mitochondrial fractions (25 μg protein) were assayed for activity spectrophotometrically at 600 nm, in 1 mL of a reaction medium containing 0.05 M potassium phosphate pH 7.5, 90 μM ubiquinone 2 (UQ$_2$, Sigma-Aldrich), 55 μM dichlorophenolindophenol (DCIP; Merck; extinction coefficient 21 mM^{-1} cm^{-1}), and 0.01 M sodium succinate (Merck). The reaction was performed at 30°C for 30 min, conditions in which DCIP reduction was proportional to incubation time and protein concentration.

Microscopic Analysis

Alexander staining of pollen was performed by incubating anthers from recently opened flowers in Alexander's solution for 15 min (Alexander, 1969; Johnson-Brousseau and McCormick, 2004). For anther structure analysis, flowers were fixed overnight in 3% (v/v) glutaraldehyde, 0.1 M sodium cacodylate, pH 7.2, dehydrated in acetone series to 100%, and embedded in Embed812 resin according to the recommendations of the manufacturer (EMS). Anther transverse sections (2 μm) were stained with 1% toluidine blue. Alexander stained pollen and anther cross sections were viewed using a light

microscope (Optiphot-2, Nikon), and bright-field photographs were taken with a Nikon Coolpix 4500 CCD digital camera.

For transmission electron microscopy, samples were fixed in 3% (v/v) glutaraldehyde, 0.1 M sodium cacodylate, pH 7.2, and postfixed in 1% osmium tetroxide for 1 h, dehydrated in a graduate acetone series, embedded in Epon resin, and polymerized at 60°C for 24 h. Ultrathin sections (60 nm) were cut with a diamond knife (Micro Star) on a Sorvall MT-5000 microtome and mounted on 300 mesh copper grids. Sections were stained with 4% (w/v) uranyl acetate and lead citrate in methanol (Reynolds, 1963) and viewed with a Philips Tecnai 12 Bio Twin transmission electron microscope operating at 80 kV. Micrographs were taken using Kodak Electron Image SO163 film (Kodak).

To analyze the terminal phenotype of ovules, flowers were emasculated and ovules observed 48 h after emasculation. For this, wild-type and mutant pistils were dissected longitudinally with hypodermic needles, fixed overnight at room temperature in 50% (v/v) ethanol, 5% (v/v) glacial acetic acid, 10% (v/v) formaldehyde, and then cleared in chloral hydrate:glycerol:water (8g:2 mL:1 mL). Single ovules were dissected and viewed with a light microscope (Optiphot-2, Nikon) equipped for differential interference contrast (DIC). Images were captured using a Nikon Coolpix 4500 CCD digital camera.

Generation of ihpRNA Lines

A 225-bp fragment containing the 5' UTR and the first exon of *SDH1-1* was PCR amplified using the forward primer 5' *AAGCAGGCT*ACTAGTGTT-CGCGTCTTCCT 3' and the reverse primer 5' *CAAGAAAGCT*GGGTAGAAC-CAGTGGAGA 3' (partial attB sites in italics, *Spe*I restriction site underlined). The resulting product, which contained at both ends partial attB recombination sites of the Gateway system (Invitrogen), was reamplified using primers attB1 (5' GGGGACAAGTTTGTACAAAAAAGCAGGCT 3') and attB2 (5' GGGGACCACTTTGTACAAGAAAGCTGGGT 3'). The PCR product (*attB1:SDH1-1:attB2*) was cloned into a pGEM-T easy vector (Promega) and sequenced. An in vitro recombination reaction was performed according to the manufacturer's protocol, using BP Clonase (Invitrogen), the vector pHELLSGATE4 (Helliwell et al., 2002), and gel-purified *attB1:SDH1-1:attB2* DNA fragment. Spectinomycin-resistant *Escherichia coli* XL-1blue colonies bearing the recombinant plasmid were selected. The resulting plasmid, containing *SDH1-1* sequences in both sense and antisense orientations separated by a pyruvate orthophosphate dikinase intron and under the control of the cauliflower mosaic virus 35S promoter, was transferred to *Agrobacterium tumefaciens* C58. *A. tumefaciens*-mediated transformation of Arabidopsis Columbia 0 plants was accomplished using the floral dip protocol (Clough and Bent, 1998). Seeds of the T_1 generation were selected for resistance to kanamycin.

Supplemental Data

The following materials are available in the online version of this article.

Supplemental Figure S1. *SDH1-1* and *SDH1-2* expression in different tissues and developmental stages.

Supplemental Figure S2. Expression of the complex II genes during pollen development.

Supplemental Table S1. Segregation analysis of *sdh1-1*.

Supplemental Table S2. TE of *sdh1-1* in reciprocal crosses.

Supplemental Table S3. Frequency of aborted pollen in *SDH1-1/sdh1-1* plants.

LITERATURE CITED

Alexander MP (1969) Differential staining of aborted and non-aborted pollen. Stain Technol **44:** 117–122

Alonso JM, Stepanova AN, Leisse TJ, Kim CJ, Chen H, Shinn P, Stevenson DK, Zimmerman J, Barajas P, Cheuk R, et al (2003) Genome-wide insertional mutagenesis of *Arabidopsis thaliana*. Science **301:** 653–657

Ausubel FM, Brent R, Kingston RE, Moore DD, Seidman JG, Smith JA, Struhl K (1994) Current Protocols in Molecular Biology. Wiley Interscience, New York

Bourgeron T, Rustin P, Chretien D, Birch-Machin M, Bourgeois M, Viegas-Péquignot E, Munnich A, Rötig A (1995) Mutation of a nuclear succinate dehydrogenase gene results in mitochondrial respiratory chain deficiency. Nat Genet **11:** 144–149

Boyes DC, Zayed AM, Ascenzi R, McCaskill AJ, Hoffman NE, Davis KR, Görlach J (2001) Growth stage-based phenotypic analysis of Arabidopsis: a model for high throughput functional genomics in plants. Plant Cell **13:** 1499–1510

Bradford MM (1976) A rapid and sensitive method for the quantitation of microgram quantities of protein utilizing the principle of protein-dye binding. Anal Biochem **72:** 248–254

Carrari F, Nunes-Nesi A, Gibon Y, Lytovchenko A, Ehlers Loureiro M, Fernie AR (2003) Reduced expression of aconitase results in an enhanced rate of photosynthesis and marked shifts in carbon partitioning in illuminated leaves of wild species tomato. Plant Physiol **133:** 1322–1335

Christensen CA, Gorsich SW, Brown RH, Jones LG, Brown J, Shaw JM, Drews GN (2002) Mitochondrial *GFA2* is required for synergid cell death in Arabidopsis. Plant Cell **14:** 2215–2232

Clough SJ, Bent AF (1998) Floral dip: a simplified method for *Agrobacterium*-mediated transformation of *Arabidopsis thaliana*. Plant J **16:** 735–743

De Buck S, Jacobs A, Van Montagu M, Depicker A (1999) The DNA sequences of T-DNA junctions suggest that complex T-DNA loci are formed by a recombination process resembling T-DNA integration. Plant J **20:** 295–304

De Neve M, De Buck S, Jacobs A, Van Montagu M, Depicker A (1997) T-DNA integration patterns in co-transformed plant cells suggest that T-DNA repeats originate from co-integration of separate T-DNAs. Plant J **11:** 15–29

Drews GN, Yadegari R (2002) Development and function of the angiosperm female gametophyte. Annu Rev Genet **36:** 99–124

Dutilleul C, Driscoll S, Cornic G, De Paepe R, Foyer CH, Noctor G (2003a) Functional mitochondrial complex I is required by tobacco leaves for optimal photosynthetic performance in photorespiratory conditions and during transients. Plant Physiol **131:** 264–275

Dutilleul C, Garmier M, Noctor G, Mathieu C, Chétrit P, Foyer CH, De Paepe R (2003b) Leaf mitochondria modulate whole cell redox homeostasis, set antioxidant capacity, and determine stress resistance through altered signaling and diurnal regulation. Plant Cell **15:** 1212–1226

Elorza A, León G, Gómez I, Mouras A, Holuigue L, Araya A, Jordana X (2004) Nuclear *SDH2-1* and *SDH2-2* genes, encoding the iron-sulfur subunit of mitochondrial complex II in Arabidopsis, have distinct cell-specific expression patterns and promoter activities. Plant Physiol **136:** 4072–4087

Elorza A, Roschzttardtz H, Gómez I, Mouras A, Holuigue L, Araya A, Jordana X (2006) A nuclear gene for the iron-sulfur subunit of mitochondrial complex II is specifically expressed during Arabidopsis seed development and germination. Plant Cell Physiol **47:** 14–21

Figueroa P, León G, Elorza A, Holuigue L, Araya A, Jordana X (2002) The four subunits of mitochondrial respiratory complex II are encoded by multiple nuclear genes and targeted to mitochondria in *Arabidopsis thaliana*. Plant Mol Biol **50:** 725–734

Figueroa P, León G, Elorza A, Holuigue L, Jordana X (2001) Three different genes encode the iron-sulfur subunit of succinate dehydrogenase in *Arabidopsis thaliana*. Plant Mol Biol **46:** 241–250

Gibeaut DM, Hulett J, Cramer GR, Seemann JR (1997) Maximal biomass of *Arabidopsis thaliana* using a simple, low-maintenance hydroponic method and favorable environmental conditions. Plant Physiol **115:** 317–319

Gutierres S, Sabar M, Lelandais C, Chétrit P, Diolez P, Degand H, Boutry M, Vedel F, de Kouchkovsky Y, De Paepe R (1997) Lack of mitochondrial and nuclear-encoded subunits of complex I and alteration of the respiratory chain in *Nicotiana sylvestris* mitochondrial deletion mutants. Proc Natl Acad Sci USA **94:** 3436–3441

Hanson MR, Bentolila S (2004) Interactions of mitochondrial and nuclear genes that affect male gametophyte development. Plant Cell (Suppl) **16:** S154–169

Heiser V, Brennicke A, Grohmann L (1996) The plant mitochondrial 22 kDa (PSST) subunit of respiratory chain complex I is encoded by a nuclear gene with enhanced transcript levels in flowers. Plant Mol Biol **31:** 1195–1204

Helliwell CA, Wesley SV, Wielopolska AJ, Waterhouse PM (2002) High-throughput vectors for efficient gene silencing in plants. Funct Plant Biol **29:** 1217–1225

Honys D, Twell D (2004) Transcriptome analysis of haploid male gametophyte development in *Arabidopsis*. Genome Biol **5:** R85

Howden R, Park SK, Moore JM, Orme J, Grossniklaus U, Twell D (1998) Selection of T-DNA-tagged male and female gametophytic mutants by segregation distortion in Arabidopsis. Genetics **149:** 621–631

Huang J, Friedhelm S, Matzinger DF, Levings CS III (1994) Flower-enhanced expression of a nuclear-encoded mitochondrial respiratory protein is associated with changes in mitochondrion number. Plant Cell **6:** 439–448

Johnson-Brousseau SA, McCormick S (2004) A compendium of methods useful for characterizing *Arabidopsis* pollen mutants and gametophytically-expressed genes. Plant J **39:** 761–775

Landschütze V, Willmitzer L, Müller-Rober B (1995) Inhibition of flower formation by antisense repression of mitochondrial citrate synthase in transgenic potato plants leads to a specific disintegration of the ovary tissues of flowers. EMBO J **14:** 660–666

Lee B, Lee H, Xiong L, Zhu J-K (2002) A mitochondrial complex I defect impairs cold-regulated nuclear gene expression. Plant Cell **14:** 1235–1251

Lee SLJ, Warmke HE (1979) Organelle size and number in fertile and T-cytoplasmic male-sterile corn. Am J Bot **60:** 141–148

Lemire BD, Oyedotun KS (2002) The *Saccharomyces cerevisiae* mitochondrial succinate: ubiquinone oxidoreductase. Biochim Biophys Acta **1553:** 102–116

Lin M, Behal RH, Oliver DJ (2004) Characterization of a mutation in the IDH-II subunit of the NAD$^+$-dependent isocitrate dehydrogenase from *Arabidopsis thaliana*. Plant Sci **166:** 983–988

McCormick S (2004) Control of male gametophyte development. Plant Cell (Suppl) **16:** S142–S153

Meyers BC, Vu TH, Tej SS, Ghazal H, Matvienko M, Agrawal V, Ning J, Haudenschild CD (2004) Analysis of the transcriptional complexity of *Arabidopsis thaliana* by massively parallel signature sequencing. Nat Biotechnol **22:** 1006–1011

Millar HA, Eubel H, Jänsch L, Kruft V, Heazlewood JL, Braun HP (2004) Mitochondrial cytochrome c oxidase and succinate dehydrogenase complexes contain plant specific subunits. Plant Mol Biol **56:** 77–90

Miyadera H, Shiomi K, Ui H, Yamaguchi Y, Masuma R, Tomoda H, Miyoshi H, Osanai A, Kita K, Omura S (2003) Atpenins, potent and specific inhibitors of mitochondrial complex II (succinate-ubiquinone oxidoreductase). Proc Natl Acad Sci USA **100:** 473–477

Niewiadomski P, Knappe S, Geimer S, Fischer K, Schulz B, Unte US, Rosso MG, Ache P, Flügge U-I, Schneider A (2005) The Arabidopsis plastidic glucose 6-phosphate/phosphate translocator GPT1 is essential for pollen maturation and embryo sac development. Plant Cell **17:** 760–775

Nunes-Nesi A, Carrari F, Lytovchenko A, Smith AMO, Ehlers Loureiro M, Ratcliffe RG, Sweetlove LJ, Fernie AR (2005) Enhanced photosynthetic performance and growth as a consequence of decreasing mitochondrial malate dehydrogenase activity in transgenic tomato plants. Plant Physiol **137:** 611–622

Owen HA, Makaroff CA (1995) Ultrastructure of microsporogenesis and microgametogenesis in *Arabidopsis thaliana* (L.) Heynh. ecotype Wassilewskija (Brassicaceae). Protoplasma **185:** 7–21

Pagnussat GC, Yu H-J, Ngo QA, Rajani S, Mayalagu S, Johnson CS, Capron A, Xie L-F, Ye D, Sundaresan V (2005) Genetic and molecular identification of genes required for female gametophyte development and function in *Arabidopsis*. Development **132:** 603–614

Park SK, Howden R, Twell D (1998) The *Arabidopsis thaliana* gametophytic mutation *gemini pollen1* disrupts microspore polarity, division asymmetry and pollen cell fate. Development **125:** 3789–3799

Piruat JI, Pintado CO, Ortega-Sáenz P, Roche M, López-Barneo J (2004) The mitochondrial *SDHD* gene is required for early embryogenesis, and its partial deficiency results in persistent carotid body glomus cell activation with full responsiveness to hypoxia. Mol Cell Biol **24:** 10933–10940

Pla M, Mathieu C, De Paepe R, Chétrit P, Vedel F (1995) Deletion of the last two exons of the mitochondrial *nad7* gene results in lack of the NAD7 polypeptide in a *Nicotiana sylvestris* CMS mutant. Mol Gen Genet **248:** 79–88

Portereiko MF, Sandaklie-Nikolova L, Lloyd A, Dever CA, Otsuga D, Drews GN (2006) *NUCLEAR FUSION DEFECTIVE1* encodes the Arabidopsis RPL21M protein and is required for karyogamy during female gametophyte development and fertilization. Plant Physiol **141:** 957–965

Reynolds ES (1963) The use of lead citrate at high pH as an electron-opaque stain in electron microscopy. J Cell Biol **17:** 208–212

Rustin P, Rötig A (2002) Inborn errors of complex II—unusual human mitochondrial diseases. Biochim Biophys Acta **1553:** 117–122

Sabar M, De Paepe R, de Kouchkovsky Y (2000) Complex I impairment, respiratory compensations, and photosynthetic decrease in nuclear and mitochondrial male sterile mutants of *Nicotiana sylvestris*. Plant Physiol **124:** 1239–1250

Sanders PM, Bui AQ, Weterings K, McIntire KN, Hsu Y-C, Lee PY, Truong MT, Beals TP, Goldberg RB (1999) Anther developmental defects in *Arabidopsis thaliana* male-sterile mutants. Sex Plant Reprod **11:** 297–322

Scheffler IE (1998) Molecular genetics of succinate:quinone oxidoreductase in eukaryotes. Progr Nucleic Acid Res Mol Biol **60:** 267–315

Schmid M, Davison TS, Henz SR, Pape UJ, Demar M, Vingron M, Schölkopf B, Weigel D, Lohmann JU (2005) A gene expression map of *Arabidopsis thaliana* development. Nat Genet **37:** 501–506

Sessions A, Burke E, Presting G, Aux G, McElver J, Patton D, Dietrich B, Ho P, Bacwaden J, Ko C, et al (2002) A high-throughput Arabidopsis reverse genetics system. Plant Cell **14:** 2985–2994

Smart CJ, Monéger F, Leaver CJ (1994) Cell-specific regulation of gene expression in mitochondria during anther development in sunflower. Plant Cell **6:** 811–825

Smith NA, Singh SP, Wang M-B, Stoutjesdijk PA, Green AG, Waterhouse PM (2000) Total silencing by intron-spliced hairpin RNAs. Nature **407:** 319–320

Sussman MR, Amasino RM, Young JC, Krysan PJ, Austin-Phillips S (2000) The Arabidopsis knockout facility at the University of Wisconsin-Madison. Plant Physiol **124:** 1465–1467

Tadege M, Kuhlemeier C (1997) Aerobic fermentation during tobacco pollen development. Plant Mol Biol **35:** 343–354

Yadegari R, Drews GN (2004) Female gametophyte development. Plant Cell (Suppl) **16:** S133–S141

Yankovskaya V, Horsefield R, Törnroth S, Luna-Chavez C, Miyoshi H, Léger C, Byrne B, Cecchini G, Iwata S (2003) Architecture of succinate dehydrogenase and reactive oxygen species generation. Science **299:** 700–704

Zimmermann P, Hirsch-Hoffmann M, Hennig L, Gruissem W (2004) Genevestigator: Arabidopsis microarray database and analysis toolbox. Plant Physiol **136:** 2621–2632